Performance of Self-Supervised Model Fitting of VERDICT MRI Parameters in the Prostate

Snigdha Sen[1], Saurabh Singh[2], Hayley Pye[3], Caroline Moore[4], Hayley Whitaker[3], Shonit Punwani[2], David Atkinson[2], Eleftheria Panagiotaki[1] and Paddy J. Slator[1]

[1]*Centre for Medical Image Computing and Department of Computer Science, University College London, London, UK.* [2]*Centre for Medical Imaging, University College London, London, UK.* [3]*Molecular Diagnostics and Therapeutics Group, University College London, London, UK. Department of Urology,* [4]*University College London Hospitals NHS Foundations Trust.*

Synopsis

Diffusion-weighted MRI (DW-MRI) models are traditionally fitted via a computationally expensive non-linear least squares approach. Recent work has moved to fitting these models using supervised deep learning algorithms trained on synthetic datasets, whose underlying distribution can affect parameter estimation. Self-supervised learning may address this by extracting training labels directly from the input data. We use these three strategies to fit a complex biophysical model – the VERDICT-MRI model for prostate – and find improved performance in parameter estimation using self-supervised model fitting on simulated data. We also observe plausible tumour contrast on in-vivo prostate data, motivating the use of this novel technique.

Summary of Main Findings

DW-MRI model fitting of the VERDICT model for prostate using a self-supervised neural network improves parameter estimation over supervised deep learning and non-linear least squares fitting, and shows reasonable tumour contrast on in-vivo prostate data.

Introduction

Microstructure imaging combines bespoke diffusion-weighted MRI (DW-MRI) acquisitions with biophysical models to investigate the sub-voxel tissue microstructure. These models are traditionally fitted using a non-linear least squares (NLLS) approach. Recent work has used supervised deep learning approaches to fit these models (1) (2). However, these are typically trained on large synthetic datasets, whose underlying distribution can introduce bias into fitted parameter estimates (3). Self-supervised learning has the potential to address this issue by extracting training labels directly from the input data but can also lead to higher variance (4).

Self-supervised model fitting has been used successfully to improve microstructural parameter estimation for two-compartment models (5) (4) (6). This work is the first to trial this approach for three-compartment (or higher) models, or for the prostate. We compare three model fitting strategies – NLLS, supervised learning, and self-supervised learning – for the VERDICT-MRI model (7) (8) (9), both in simulations and in in-vivo prostate. Results show that self-supervised learning improves performance on simulated data compared to NLLS and MLP and yields maps retaining? tumour contrast on in-vivo scans.

Methods

Simulated Dataset
10,000 DW-MRI signals were simulated to quantitatively assess the performance of the self-supervised fitting against NLLS and MLP. The same acquisition parameters were used as in patient datasets, and parameter values were randomly sampled (using a uniform distribution) from biophysically plausible parameter ranges: f_{IC}, f_{EES}: [0,1], R: [0,15]μm and

d_{EES}: [0.5,3] $\mu m^2/ms$, with the constraint $f_{IC} + f_{EES} + f_{VASC} = 1$. Rician noise was also added, with SNR = 50.

Data Acquisition

Four men with biopsy-confirmed clinically significant prostate cancer from the INNOVATE clinical trial (10) were analysed in this study. VERDICT-MRI data was acquired on a 3T scanner (Achieva, Philips Healthcare, Best, Netherlands), with a pulsed-gradient spin echo () sequence. Imaging parameters were: TR/TE, 2482–3945/50–90; field of view, 220 × 220 mm; section thickness, 5 mm; no intersection gap; acquisition matrix, 176 × 176; in-plane resolution, 1.25 × 1.25 mm; b-values, 90, 500, 1500, 2000, and 3000 s/mm^2. Each b-value also included a b=0 image using the same TE as the corresponding diffusion weighted image. The total imaging time was 12 minutes (11).

Biophysical Model

The VERDICT prostate model has three compartments characterising diffusion in the vascular (VASC), extracellular-extravascular space (EES) and intracellular (IC) components in tumours. These are modelled as randomly-oriented sticks (AstroSticks), Gaussian free diffusion (Ball) and restriction in an impermeable sphere (Sphere) respectively (7). We estimate four model parameters: f_{IC} (IC volume fraction), f_{EES} (EES volume fraction), cell radius R and EES diffusivity d_{EES} (12) (13). The vascular volume fraction is calculated as $f_{VASC} = 1 - f_{IC} - f_{EES}$. The DW-MRI signal for VERDICT is:

$S(b)/S_0 = f_{VASC}S_{VASC}(d_{VASC},b) + f_{IC}S_{IC}(d_{IC},R,b) + f_{EES}S_{EES}(d_{EES},b)$

where b is the b-value and S_0 is the b=0 signal intensity.

Parameter Estimation

We consider three approaches: i) NLLS estimation, ii) supervised deep learning with multilayer perceptron (MLP) (1) consisting of three fully-connected hidden layers, each with 150 neurons, trained on 100,000 synthetic DW-MRI signals with added Rician noise (2) and iii) a novel self-supervised (SS) deep learning technique using a feed-forward, back propagation fully-connected neural network (FCNN) (3). The network consists of an input layer and three fully-connected hidden layers (each with 10 neurons to match the number of diffusion-weighted acquisition volumes) and an output layer with four neurons, one for each of the parameters to be estimated. A schematic representation of the self-supervised technique is given in Figure 1.

Results

Table 1 shows mean squared error (MSE) values obtained between parameter estimates and ground truth values for all three fitting strategies on simulated data. We find that self-supervised fitting produces the lowest MSE across all four VERDICT parameters. Scatter plots of parameter estimates obtained using all three strategies against ground truth values are shown in Figure 2. Visually there is stronger correlation between estimates and ground truth using self-supervised fitting. This is supported by the Pearson correlation coefficients shown both on Figure 2 and in Table 1, which are higher for self-supervised fitting than for both other methods for f_{IC}, R and d_{EES}.

Examplar maps from a patient with all fitting strategies are shown in Figure 3. Self-supervised fitting produces maps with reasonable tumour contrast on in-vivo prostate data, which was observed across all four patient datasets. Some further hyperparameter tuning is necessary to achieve the detail seen in NLLS maps.

Discussion and Conclusion

This work presents a comparison between three DW-MRI model-fitting strategies: NLLS, supervised deep learning via MLP and a novel self-supervised FCNN approach. Self-supervised fitting demonstrates improved performance over MLP and NLLS fitting on simulated data, in terms of MSE and Pearson correlation coefficient. VERDICT maps on in-vivo prostate data show reasonable tumour contrast, but are less detailed, indicating further tuning of the network is needed for reliable performance on real MRI data. This is likely due the complexity of the signal from the Sphere compartment.

Future work will quantitatively compare the fitting strategies in more detail by considering bias and variance separately. We will also analyse their performance on a larger patient cohort in delineating different tissue types, and explore the generalisability of self-supervised learning to unseen data.

Bibliography

1. Golkov V, Dosovitskiy A, Sperl JI, Menzel MI, Czisch M, Samann P, et al. q-Space Deep Learning: Twelve-Fold Shorter and Model-Free Diffusion MRI Scans. IEEE Trans Med Imaging. 2016 May; 35(5): p. 1344-1351.

2. Valindria V, Chiou E, Palombo M, Singh S, Punwani S, Panagiotaki E. Synthetic q-space learning with deep regression networks for prostate cancer characterisation with VERDICT. In IEEE International Symposium on Biomedical Imaging (ISBI); 2021.

3. Gyori NG, Palombo M, Clark CA, Zhang H, Alexander DC. Training data distribution significantly impacts the estimation of tissue microstructure with machine learning. Magn Reson Med. 2021; 87: p. 932-947.

4. Epstein SC, Bray TJP, Hall-Craggs M, Zhang H. Choice of training label matters: how to best use deep learning for quantitative MRI parameter estimation. ArXiv Preprint. 2022 May.

5. Barbieri S, Gurney-Champion OJ, Klaassen R, Thoeny HC. Deep learning how to fit an intravoxel incoherent motion model to diffusion-weighted MRI. Magn Reson Med. 2020 Jan; 83(1): p. 312-321.

6. Lim JP, Blumberg SB, Narayan N, Epstein S, Alexander DC, Palombo M, et al. Fitting a Directional Microstructure Model to Diffusion-Relaxation MRI Data with Self-Supervised Machine Learning. ArXiv Preprint. 2022 Oct.

7. Panagiotaki E, Chan RW, Dikaios N, Ahmed HU, O'Callaghan J, Freeman A, et al. Microstructural characterization of normal and malignant human prostate tissue with vascular, extracellular, and restricted diffusion for cytometry in tumours magnetic resonance imaging. Invest Radiol. 2015 Apr; 50(4): p. 218-27.

8. Johnston EW, Bonet-Carne E, Ferizi U, Yvernault B, Pye H, Patel D, et al. VERDICT MRI for Prostate Cancer: Intracellular Volume Fraction versus Apparent Diffusion Coefficient. Radiology. 2019 Apr; 291(2): p. 391-397.

9. Singh S, Rogers H, Kanber B, Clemente J, Pye H, Johnston E, et al. Avoiding Unnecessary Biopsy after Multiparametric Prostate MRI with VERDICT Analysis: The INNOVATE Study. Radiology. 2022 Aug.

10. Johnston E, Pye H, Bonet-Carne E, Panagiotaki E, Patel D, Galazi M, et al. INNOVATE: A prospective cohort study combining serum and urinary biomarkers with novel diffusion-weighted magnetic resonance imaging for the prediction and characterization of prostate cancer. BMC Cancer. 2016 Oct; 16(1): p. 816.

11. Panagiotaki E, Ianus A, Johnston E, Chan RW, Stevens N, Atkinson D, et al. Optimised VERDICT-MRI protocol for prostate cancer characterisation. In International Society for Magnetic Resonance in Medicine (ISMRM); 2015.

12. Bonet-Carne E, Johnston E, Daducci A, Jacobs JG, Freeman A, Atkinson D, et al. VERDICT-AMICO: Ultrafast fitting algorithm for non-invasive prostate microstructure characterization. NMR Biomed. 2019 Jan; 32(1).

13. Sen S, Valindria V, Slator PJ, Pye H, Grey A, Freeman A, et al. Differentiating False Positive Lesions from Clinically Significant Cancer and Normal Prostate Tissue Using VERDICT MRI and Other Diffusion Models. Diagnostics. 2022 Jul; 12(7).

14. Panagiotaki E, Walker-Samuel S, Siow B, Johnson SP, Rajkumar V, Pedley RB, et al. Noninvasive quantification of solid tumor microstructure using VERDICT MRI. Cancer Res. 2014 Apr; 74(7): p. 1902-12.
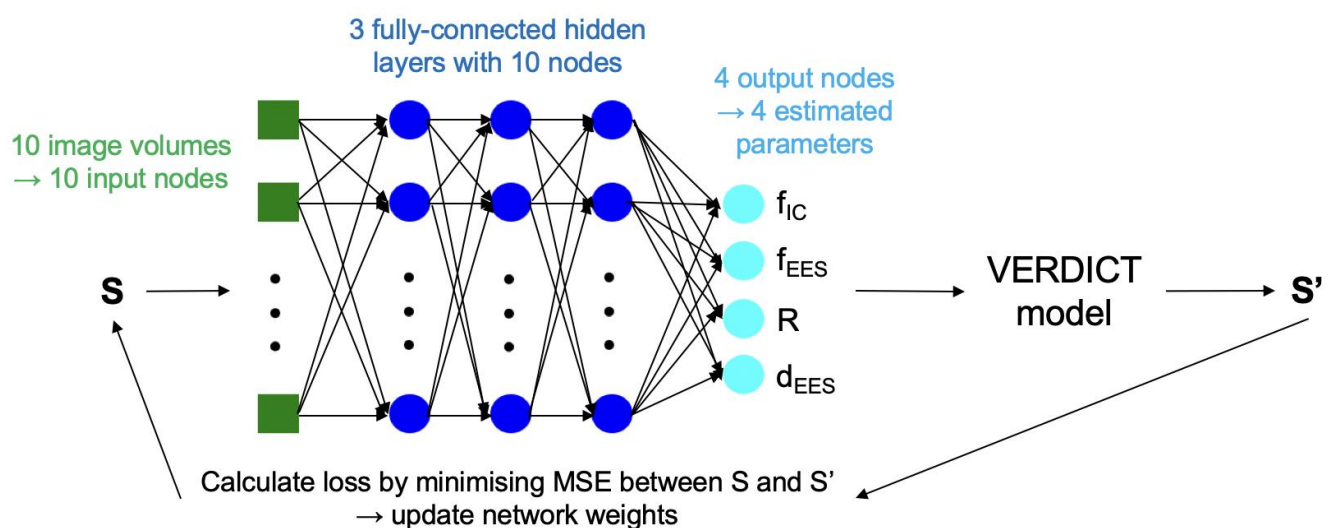
Figures

Figure 1: Schematic representation of self-supervised model fitting strategy. 10 image volumes are inputted into the network (five b=0 and one directionally-averaged image for

each b-value). There are three fully-connected hidden layers, each with 10 nodes and then a final output layer of four nodes, one for each parameter to be estimated. These parameters are then fed into the VERDICT signal model to create the reconstructed signal, S'. The loss is computed by minimising the mean-squared error (MSE) between the input signal, S and S'. This is then used to adjust the weights of the network.

	fIC	fEES	R	dEES
SS r	**0.8225**	0.6124	**0.8188**	**0.4050**
SS MSE	**0.0001**	**0.0001**	**0.0266**	**0.0025**
NLLS r	0.7932	**0.6456**	0.5803	0.3900
NLLS MSE	0.0002	**0.0001**	0.0745	0.0029
MLP r	0.5854	0.4828	0.5650	0.1960
MLP MSE	0.0002	0.0002	0.0655	0.0026

Table 1: Pearson correlation coefficients (r) and mean-squared errors (MSE) for parameter estimates from each model. We observe lowest MSE across all fitted parameters for self-supervised fitting, and highest correlation for fIC, fEES and dEES.
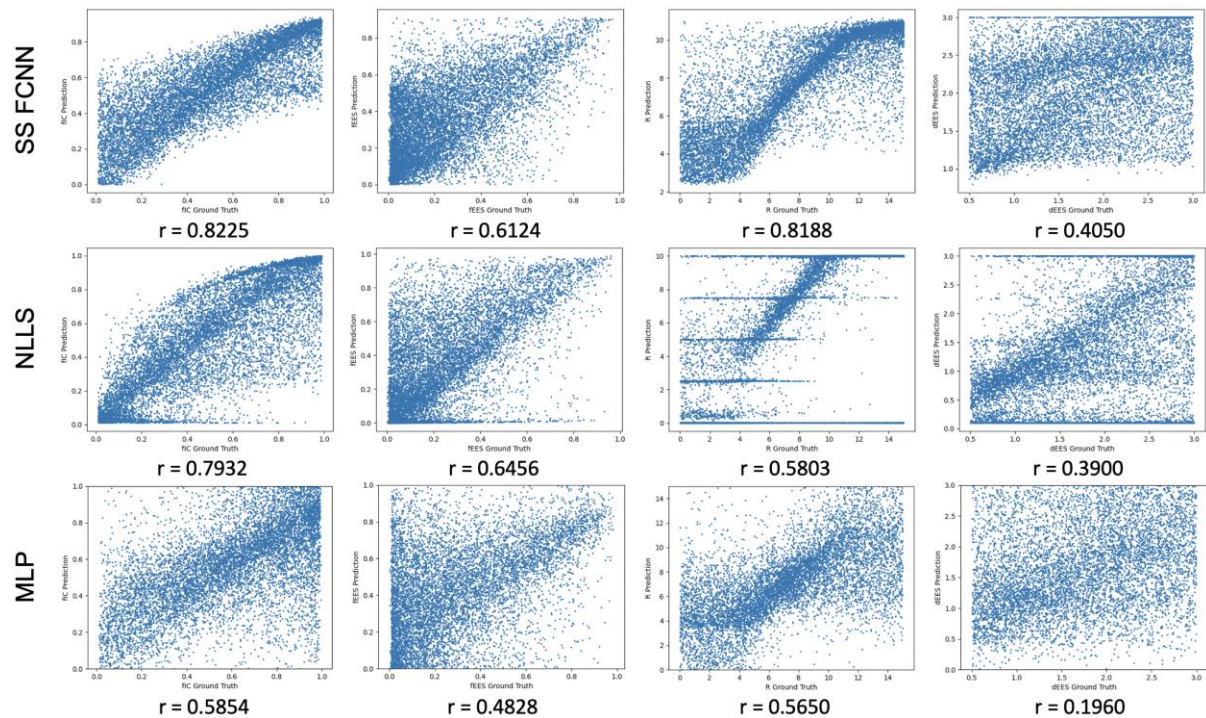

Figure 2: Scatter plots comparing performance of self-supervised fitting (SS FCNN) against NLLS and MLP. Ground truth parameters were those used to simulate the signals. Pearson correlation coefficients are shown below each parameter. Visually, strong correlation is observed for self-supervised fitting. f_{IC}, R and d_{EES} have higher Pearson correlation coefficient when fitted using self-supervised learning than with NLSS and MLP.
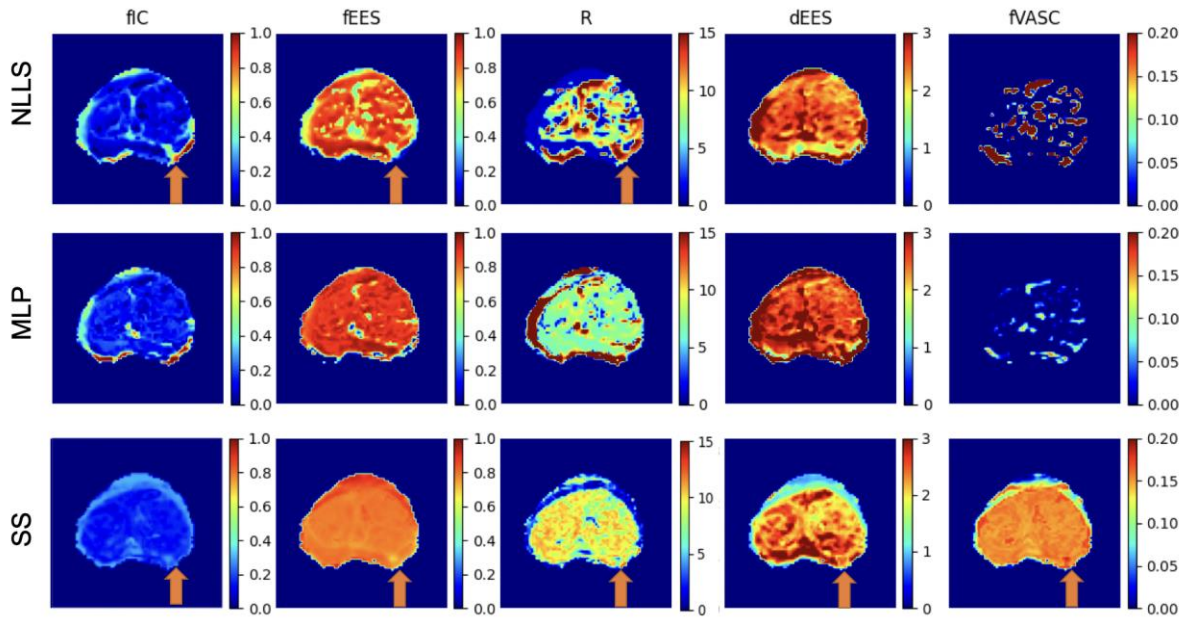
Figure 3: Parametric maps obtained from one example patient dataset using the three fitting strategies. Arrows highlight the cancerous lesion where it is shown clearly on parametric maps. We find reasonable tumour contrast using self-supervised fitting, but further network tuning is necessary to achieve more detail in f_{IC} and f_{EES} maps.